manent thermocline. In the warm season, the same layers may be secluded from direct interchange with the air by the stable stratification of the seasonal thermocline. This process is not only of interest for the formation of different water masses, but also for exchange of properties between atmosphere and ocean, e.g., gas exchange. Gas, for example oxygen or CO_2, may enter the ocean from the atmosphere by diffusion processes through the interface. It is then mixed throughout the mixed layer at the top of the ocean. Further downward transport is small due to the stable stratification. The ventilation process provides for transport to deeper layers at least during parts of the year.

Previously only very coarse estimates of the heat exchange at the air-sea interface have been available. From a data set of 8 million observations reported by voluntary observing ships, it has been possible to calculate the different components of the air-sea heat exchange. The data set allows a high spatial resolution [2].

Calculation of the net energy flux at the air-sea interface has been through parameterization of the main components of the energy balance: incoming short-wave radiation, depending on solar height and on cloudiness; net long-wave radiation at the sea surface, depending mainly on temperature, water vapor content and cloudiness; evaporation as function of air-sea humidity difference and wind speed; and exchange of sensible heat, depending on the air-sea temperature difference and wind speed.

Due to the different atmospheric and oceanic parameters, the pattern of seasonal variation of the zero heat flux line shows considerable detail (Fig. 1). The seasonal variation of insolation, of course, is dominated by the height of the sun, but is modified markedly by cloudiness. The second major energy component, evaporation, is strong in the tropics due to higher water temperature, and is most pronounced in the Trade Wind region and the West Wind Drift due to higher wind speeds. Combination of high evaporation and low insolation leads to an area of heat loss from the ocean to the atmosphere centered at 10° N between 35° W and 50° W, first detected by Bunker and Worthington [1]. The general equator-to-pole variation of insolation and evaporation is modified on the west side through advection by the strong currents of the Gulf Stream and North Atlantic Current, and on the east side by upwelling at the North West African coast.

In spring, heat flux from the ocean to the atmosphere is found in a band from the Gulf Stream area to the Northeast Atlantic, and in a smaller area in the Trade Wind region off South America. In the remaining regions the ocean gains heat. In summer, most of the North Atlantic Ocean gains heat except for a small area in the Gulf Stream region in August and some areas in the inner tropics, where reduced insolation and high evaporation yield a heat flux into the atmosphere. In fall, most of the northern part of the ocean loses heat to the atmosphere, while the southern regions of the ocean still gain heat. Also in September, some cold water areas, e.g. of the Labrador Current, gain heat. In winter almost the total area of the North Atlantic Ocean gives heat to the atmosphere except for the inner tropics and the waters near the African coast.

In the annual average (as shown by the dashed line in Fig. 1b) the northern part of the ocean and an area in the Trade Wind region off South America loses heat to the atmosphere, while the southern part of the ocean and the cold water areas of the Labrador Current and the West Greenland Current gain heat.

It may be mentioned that climate evaluation from ship observations is not a simple task. Since the components of heat exchange are not directly measured, the calculations involve parameterizations which are less than perfect. Ongoing research and collection of more data may perhaps yield later revisions of the present knowledge. Despite this we believe that the calculated regional and annual variation is typical, and can be used in other research even if details need to be revised. This statement is based on the fact that the systematic uncertainties involved are about 15 Wm^{-2}. The annual and regional variation of net heat exchange is several hundreds of Wm^{-2}, therefore revisions of the parameterizations should not distort the overall picture.

This research was supported by the Deutsche Forschungsgemeinschaft, SFB 133. The data used for this investigation were originally processed by A.F. Bunker of Woods Hole Oceanographic Institution.

Received January 10, 1986

1. Bunker, A.F., Worthington, L.V.: Bull. Am. Met. Soc. *57*, 670 (1976)
2. Isemer, H.J., Hasse, L.: The Bunker Climate Atlas of the North Atlantic Ocean. Berlin-Heidelberg-New York: Springer 1985
3. Woods, J.D., Barkmann, W.: Nature *319*, 574 (1986)

Removal of Strontium by Coprecipitation in Lake Constance with Calcite

H.-H. Stabel, J. Küchler-Krischun, J. Kleiner, and P. Merkel
Limnologisches Institut der Universität, D-7750 Konstanz

The Sr/Ca ratio (defined as atoms Sr/atoms Ca × 1000) in water from Lake Constance is 6 ± 0.5 [1] and thus is exceptionally high compared to most freshwaters [2]. The fact that in the main tributary (the Alpenrhein) high Sr concentrations occur together with high sulfate contents has led to the conclusion that celestite ($SrSO_4$) is leached in the drainage area. Larger quantities of celestite were reported for the northern rim of the Northern Calcareous Alps [3] especially for the Ladinian "Wettersteinkalk" which is also present in the watershed area of Lake Constance [4]. The Sr/Ca ratio of the lake is balanced mainly by the Sr content of riverine water [1]. This concentra-

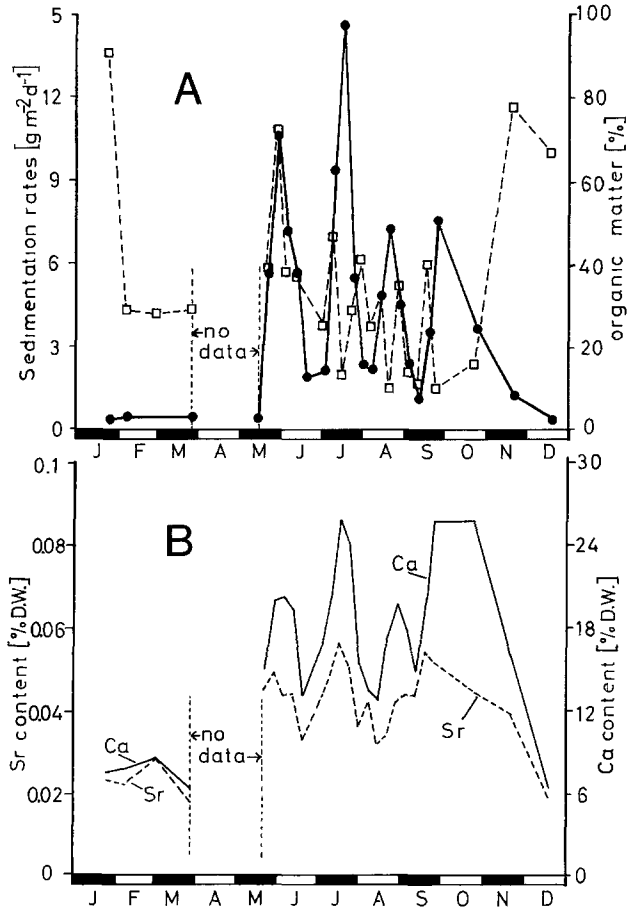

Fig. 1. A) Seasonal variations in the sedimentation rates of dry matter (●) and of organic matter (□) in the settling material; B) seasonal variations in the Sr and Ca contents of settling material in Lake Constance

tion varies seasonally between 0.35 and 0.86 mg l^{-1}, whereas strontium concentrations in the lake and in the outflow (the Seerhein) are rather constant (0.42 mg l^{-1}) either due to a dilution effect in the lake water or to the removal of Sr by precipitation. Three different sinks can be discussed: uptake by biota, adsorption to particulate matter, and coprecipitation with calcite which is authigenically formed in summer [5]. Here we report on the sedimentation of strontium and calcium measured with sedimentation traps from January 1985 to March 1986. The traps were suspended at 20 m depth (i.e., the maximum extension of the euphotic zone) and were retrieved in nearly weekly intervals. Methods of sample preparation and combustion are reported in [5, 6]. Contents of Sr and Ca were analyzed by atomic absorption spectrometry (Perkin Elmer, Mod. 3030B).

Phytoplankton is the main source of suspended particulate organic matter in the euphotic zone of Lake Constance [7]. The sedimentation rates of organic matter (Fig. 1A) vary independently from fluctuations in the algal biomass and are not correlated with the sedimentation rates of particles, expressed as dry weight (DW). There are also no relations between sedimentary fluxes of strontium and of organic material.

Calcium carbonate, on the other hand, is the major component of settling material and thus Ca fluxes seem to control the sedimentation rates of DW. The annual mean Sr/Ca ratio in the settling material of Lake Constance is 3.6. During the annual cycle there is a close linear correlation between the Ca and the Sr contents in the sedimentary matter (Fig. 1B):

$$[Sr] = 0.00165 \times [Ca] + 0.0124$$

[Sr] and [Ca] in % of DW, $n = 26$, $r = 0.804$.

From these data we suggest that there is coprecipitation of calcium and strontium in Lake Constance, while a Ca-independent precipitation of Sr (e.g., uptake by biota, binding on noncalcareous minerals) is of minor significance and can be estimated from the y-intercept of the regression line.

In order to test whether in Lake Constance strontium is removed predominantly by coprecipitation with calcite, the following experiment was performed: Lake water from 50 m depth was filtered through membrane filters of 0.2 µm pore size. In order to achieve a high degree of supersaturation, the pH of the filtrate was adjusted to 9.5 with NaOH and $CaCl_2 \cdot 2H_2O$ was added until a calcite saturation index (Ω) close to 48 was reached. According to [8], this index is defined as the ratio of the ion activity product of the solution divided by the solubility constant. The reaction was performed in a closed bottle at 15 °C. The addition of $CaCO_3$ seed crystals (10 mg l^{-1} in the reaction vessel) led to rapid calcite precipitation. Within 14 h the pH was lowered to 9.2 and the Ca concentration was reduced from 1.215×10^{-3} to 0.854×10^{-3} mol l^{-1} (cf. Table 1). Concomitantly, the Sr concentration decreased from 5.17×10^{-6} to 4.54×10^{-6} mol l^{-1}. In the solute the Sr/Ca ratio increased from 4.26 to 5.32 (values slightly lower than in [1] because of the addition of $CaCl_2$). In the precipitates, however, the ratio is calculated to 1.72, a value which is nearly 50% of the annual

Table 1. Experimental data of the calcite precipitation experiments (Ω = calcite saturation index, see text)

pH_{start}	pH_{end}	$[Ca]_{start}$	$[Ca]_{end}$	$[Sr]_{start}$	$[Sr]_{end}$	Ω_{start}	Ω_{end}
		[10^{-3} mol l^{-1}]		[10^{-6} mol l^{-1}]			
9.51	9.21	1.157	0.853	5.02	4.57	45.33	16.25
9.53	9.21	1.18	0.838	5.14	4.45	46.87	17.14
9.5	9.19	1.309	0.869	5.36	4.57	50.7	15.46

mean ratio determined by sedimentation trap measurements in the lake.

Although these experiments clearly prove coprecipitation of Sr with calcite, constant stoichiometric relations cannot be derived from the preliminary data as yet. Nevertheless, both field data and laboratory experiments show that coprecipitation is a significant sink of strontium in Lake Constance. The relevance of Ca and Sr sedimentation for the whole lake budgets of these elements is presently under study.

This work was supported by the Deutsche Forschungsgemeinschaft (DFG-Az.: Sta 197/4).

Received March 11 and April 28, 1986

1. Müller, G.: Miner. Deposita *4*, 75 (1969)
2. Odum, H.T.: Science *114*, 407 (1951)
3. Ney, P.: Aufschluss *8*, 153 (1957)
4. Steinmetz, H.: Miner. Petrog. *1*, 399 (1948)
5. Stabel, H.-H.: Limnol. Oceanogr. (in press)
6. Stabel, H.-H., in: Chemical Processes in Lakes (W. Stumm, ed.). New York: Wiley 1985
7. Stabel, H.-H.: Hydrobiologia (in press)
8. Berner, R.A.: Chemical Sedimentology. New York: McGraw-Hill 1975

Biotinylated DNA Probes: Sensitivity and Applications

R. Neumann, P. Rudloff and H.J. Eggers
Institut für Virologie der Universität, D-5000 Köln

Radioisotopes such as ^{35}S, ^{3}H, ^{125}I, ^{32}P are widely used in nucleic acid hybridization techniques. Yet they have serious limitations and disadvantages. The short functional half-life of ^{32}P-labeled DNA probes (14.3 days) is one of these restrictions. ^{3}H-labeled probes sometimes require a long time until signals can be recorded. The isotope technique is expensive (cost of isotopes and technical equipment, time required, isotope disposal) and raises safety problems; therefore, it is undesirable to use the powerful new hybridization techniques (e.g., Southern- and Northern blotting and in situ hybridization) extensively in clinical and diagnostic medicine. In medical virology, for example, it is explored whether the detection of DNA sequences of human papilloma viruses (HPV) in cervical smears may be of diagnostic and prognostic value for the recognition of development of cervical cancer [1] (see below).

In 1981, Langer and coworkers [2] reported the synthesis of nucleotide triphosphate analogs of dUTP and UTP that contain biotin covalently attached to the C-5 position of the pyrimidine ring by an allylamine arm. The nucleotide derivatives can be incorporated into nucleic acids by DNA polymerase I and serve as targets for avidin or streptavidin which show a highly specific and tenacious interaction to biotin ($K_{diss} = 10^{-15}$). When a biotinylated enzyme is added to this complex, its location can be made visible by use of an appropriate substrate which is then converted to a colored molecule.

We have tested biotin-labeled adenovirus Type 2 (Ad2) DNA probes in hybridization techniques mentioned below in order to evaluate the sensitivity of this nonradioactive labeling and detection system as compared to isotope-labeled DNA's. Adenoviral DNA was isolated as described [3]. Preparation of dot and Southern blots as well as screening of bacterial colonies was done according to routine protocols [4].

For nick translation we used standard protocols [5] with one modification. In the case of incorporation of Bio-11-dUTP higher incorporation rates were obtained using 20–50 μM of all triphosphates in the reaction.

Hybridizations were done using 10% dextran sulfate [6]. We used up to 400 ng of biotin-labeled DNA per ml of hybridization solution. Subsequently, we followed published protocols [2].

The results using the nonradioactive DNA detection system with a biotinylated Ad2 probe and those obtained with a phosphorus-labeled probe (specific activity 10^8 cpm/μg) are shown in Fig. 1. With both probes comparable sensitivities were recorded.

Biotinylated probes can be used over a long period of time (though the intensity of the reaction may weaken slightly). In the case demonstrated, the time interval between the 1st and the 10th hybridization was 3 months. Signals of biotinylated probes appeared much earlier than those labeled with ^{32}P. A limit of detection seems to be the use of 5 pg of homologous DNA (Fig. 1a).

The Southern blot hybridization technique has become increasingly important in molecular biology, e.g., to detect genes coding for RNA sequences and protein sequences, respectively, and may become a routine technique in medicine [7]. Therefore, we explored whether the nonradioactive DNA detection system could be applied for such assays. The result of a blotting experiment is shown in Fig. 2. If the amount of Ad2-DNA in the various restriction assays is low it is sometimes not possible to detect low-molecular-weight fragments (in the photograph as well as in the original filters). One explanation for this observation may be the small amount of DNA generated by restriction endonuclease enzymes: if 50 pg Ad2-DNA are being restricted, pieces in the range of 5 pg will ensue. Furthermore, one has to consider unpredictable transfer processes. Charged Nylon membranes such as Nytran seem to be preferable (see Fig. 2).

Re-use of nitrocellulose membranes is limited by the fact that these filters become very brittle after repeated hybridizations. Thus, application of special types of Nylon membranes demonstrated by us should be considered.

In all our experiments application of 10% dextran sulfate in the hybridization mix increased the sensitivity of the tests (data not shown).

We also used biotinylated Ad2-DNA to screen bacterial colonies for plasmids (e.g., pBR 322) containing Ad2-DNA fragments. The positive result exhibited in Fig. 3 was confirmed by hybridization with phosphorus-labeled DNA (data not shown). In another application we have been able to demonstrate that usage of phosphorus- and